ELSEVIER

Polymer 42 (2001) 4997–5004

polymer

www.elsevier.nl/locate/polymer

Crystallization of semicrystalline block copolymers containing a glassy amorphous component

T. Shiomi[a,*], H. Tsukada[a], H. Takeshita[a], K. Takenaka[a], Y. Tezuka[b]

[a]*Department of Materials Science and Technology, Nagaoka University of Technology, 1603-1 Kamitomioka, Nagaoka, Niigata 940-2188, Japan*
[b]*Department of Organic and Polymeric Materials, Tokyo Institute of Technology, O-okayama, Meguro-ku, Tokyo 152-8552, Japan*

Received 19 October 2000; accepted 29 November 2000

Abstract

The effect of the microphase separation structure in the melt on crystallizability and crystallization kinetics was studied for poly(tetrahydrofuran)–polystyrene diblock copolymers (PTHF–PS) which has a glassy amorphous component. Four kinds of copolymers, Block 1, Block 2, Block 3 and Block 4 with PTHF compositions of 59, 51, 38 and 29 vol%, respectively, were employed and their crystallization behavior was compared with the PTHF/PS blends as well as the PTHF homopolymers. Crystallization of Block 2, Block 3 and Block 4 was much suppressed, in particular no crystallization was detected for Block 4 even in a long crystallization time and at a high supercooling degree. The blends of Block 4 with the PTHF homopolymer also did not crystallize in the total PTHF content less than about 40%. It was concluded from these results that crystallization from the semidiscontinuous microdomain such as lamellar and cylindrical ones was much suppressed and that crystallization did not occur inside the discontinuous or spherical microdomain surrounded by the glassy matrix. The Avrami exponent was extremely small for Block 2 and Block 3, which suggested that their crystallization occurred under a high spatial constraint. The linear overall rate constant of crystallization for Block 1 was smaller than the blends and homopolymers, but the apparent activation energy of crystallization of Block 1 was not so different from that of the blends and homopolymers. For Block 2 and Block 3, on the other hand, the rate constant was small and the apparent activation energy was much high. The interfacial free energy of Block 2 and Block 3 estimated using the Lauritzen–Hoffman theory was also large.

Keywords: Crystallization; Microphase separation; Poly(tetrahydrofuran)–polystyrene block copolymer

1. Introduction

Crystallization and higher-order structure formation of crystalline block copolymers have been extensively studied. Since the block copolymers crystallize from unique melt with microphase separation structure, the crystallization itself and resulting higher order structure are expected to be much affected by the microdomain structure in the melt. For the system with weakly segregated microphase structure [1–3] which is realized for the block copolymer whose order–disorder transition temperature T_{ODT} is not so higher than the melting temperature T_m, higher-order structure is restructured by crystallization to be alternating structure consisting of the crystal lamella and amorphous layer as seen in usual crystalline polymers, that is, the microphase separation structure in the melt is easily destroyed by crystallization. In the strongly segregated microphase separation [4–8] in which T_{ODT} is much higher than T_m, on the other hand, crystallization occurs within the microdomain, its structure being kept.

For the copolymers having a glassy amorphous component, the microphase separation is in the strong segregation limit except for the case that the structure of the glassy domain is discontinuous or island-like, because the amorphous microdomain is in the frozen state. Therefore, it is expected that the crystalline segments are forced to crystallize in a limited space when its domain is spherical, cylindrical and lamellar, while to do with drawing the glassy domain when the amorphous domain is island-like. The crystallization of such block copolymers has been investigated for poly(ϵ-caprolactone)–polystyrene (PCL–PS) [9–13], poly(ethylene oxide)–PS [14] and poly(tetrahydrofuran)–PMMA (PTHF–PMMA) [15–18]. It was found for the neat copolymers and their blends with the homopolymer that the degree of crystallinity (DC) was depressed in the content of the crystalline component less than ca. 50% and that crystallization was not detected in less than around 30%. However, most of these studies are on static crystallization properties and morphology, and there are few

* Corresponding author. Tel.: +81-258-47-9304; fax: +81-258-47-9300.
E-mail address: shiomi@vos.nagaokaut.ac.jp (T. Shiomi).

0032-3861/01/$ - see front matter
PII: S0032-3861(00)00894-6

reports on crystallization kinetics such as crystallization rates [10,11]. Balsam et al. [11] obtained somewhat small but not so different values of the Avrami exponent, compared with those of the PCL homopolymer, for the PCL–PS–poly(butadiene) triblock copolymers with PCL contents more than 58%. The most interesting point on crystallization kinetics is in crystallization from restricted space such as lamellar, cylindrical and spherical microdomains.

In this paper we will present kinetics in crystallization of the block copolymers having a glassy amorphous component, PTHF–PS diblock copolymers, together with crystallizability from restricted microdomains.

2. Experimental

2.1. Synthesis

PTHF–PS block copolymers were prepared by the coupling reaction between anion and cation chain ends of PTHF and PS which were obtained by living cationic opening and living anionic polymerizations, respectively. The living polymerization of the PTHF precursor was carried out in bulk at 20°C using $CF_3SO_3CH_3$ as an initiator. In a desired polymerization time, a portion of the reaction solution was moved to 10% CH_3ONa solution so that the polymerization was terminated, and simultaneously the remaining solutions was also moved to a reaction mixture containing living polystyrene to be supplied to the coupling reaction. Styrene was polymerized in the mixed solvent of THF and benzene (2:1 in volume) with *n*-butyl lithium for 15 min at −45°C, and the coupling reaction of PS with PTHF was conducted by adding the above PTHF solution to the polystyrene solution. A portion of the polymerization solution of PS was moved to the solution containing a terminator of methanol just before the addition of the PTHF solution. The termination of the coupling reaction was confirmed by disappearance of red color characteristic of the polystyryl anion. After the coupling reaction an excess amount of living PTHF was treated with CH_3ONa. The resulting copolymer was purified by repeated precipitation in the THF/cold methanol system, followed by freeze-drying from the benzene solution.

The polymer product thus obtained contained the homopolymers of PS and PTHF as well as the block copolymer. The PTHF homopolymer was removed by treatment at 45°C with ethanol which is a solvent to PTHF but a nonsolvent to PS, and then fractional precipitation was carried out by adding ethanol dropwise to 3 wt% cyclohexane solution. Finally the PTHF–PS block copolymer was isolated by the GPC column fractionation. Fig. 1 shows an example of GPC traces for the samples obtained in each step of the above fractionations.

Molecular weights of components PTHF and PS of the block copolymers were determined from GPC measurements for the respective precursor polymers removed just before the coupling reaction. Here the molecular weights of PTHF were determined with the conversion factor 0.556 for those evaluated in relative to standard polystyrene. The composition of the block copolymer estimated from the molecular weights was consistent with that obtained from 400 MHz ^{1}H NMR spectra in $CDCl_3$ at 40°C.

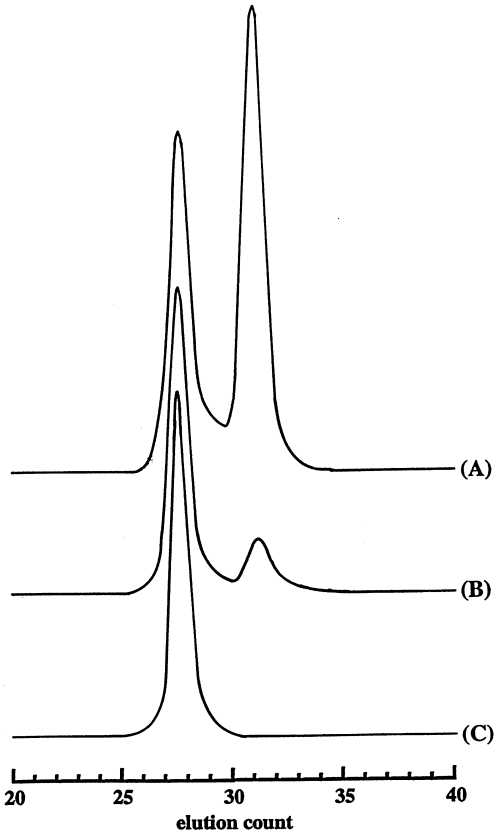

Fig. 1. GPC traces of Block 1 in each step of fractionations: (A) after treatment with ethanol; (B) after the fractional precipitation with ethanol/cyclohexane system; (C) after the GPC column fractionation.

2.2. Sample preparation and measurements

The block copolymer was dissolved in a good solvent common to both components, chloroform, to be 1 wt% solution, and then the solvent was evaporated slowly in a desiccator for 3 days at room temperature, followed by keeping in the desiccator degassed with an aspirator. Finally the samples were dried in a vacuum oven for 3 days. Furthermore, the sample was annealed under vacuum at 120°C which is higher than glass transition temperature of PS. The blend samples were prepared by the same method.

Isothermal crystallization and melting behavior were analyzed with a SEIKO I&E DSC20 differential calorimeter. In a series of thermal analyses the temperature was never raised above 60°C so that the microphase separation structure formed first could be kept. The sample was kept in a DSC apparatus for 30 min at 60°C and then rapidly cooled to a desired crystallization temperature T_c. Isothermal

Table 1
Characteristics of samples and their crystallization properties

Sample	$\bar{M}_n \times 10^{-4}$		PTHF cont.		T_c (°C)	T_m^0 (°C)	DC (%)[a]
	PS	PTHF	(Wt%)	(Vol%)[b]			
Homo 1		1.7	100	100	5.5–14.1	33.8	47
Homo 2		1.58	100	100	4.7–13.5	31.3	49
Homo 3		1.36	100	100	3.3–11.8	31.8	47
Blend 1	1.3	1.7	57	59	−1.0–7.2	30.0	34
Blend 2	1.65	1.58	49	51	−1.5–6.5	29.3	32
Blend 3	2.4	1.36	36	38	−8.3–0.0	25.7	17
Block 1	1.3	1.7	57	59	−13.3–1.3	26.8	21
Block 2	1.65	1.58	49	51	−18.1–13.4	25.1	8.4
Block 3	2.4	1.36	36	38	−21.4–13.4	25.2	3.8
Block 4	2.7	1.02	27	29	3°C/20 days	–[c]	–[c]
					−20°C/7 days	–[c]	–[c]

[a] Determined from the heat of fusion detected by DSC using the enthalpy of fusion of PTHF, $\Delta H_f = 12.4$ kJ mol^{-1} [21].
[b] Estimated using specific volumes (cm^3 g^{-1}) at 60°C; 0.9615 for glassy PS [19] and 1.044 for melt PTHF [20].
[c] No melting peak was detected by DSC.

crystallization was analyzed from an exothermal peak. After the isothermal crystallization, melting behavior was observed by heating it from T_c to 60°C at 10°C/min. The PTHF homopolymer was annealed at 60°C first, and then behavior of isothermal crystallization and melting was observed. For the block copolymers except Block 1 shown in Table 1 the isothermal crystallization was analyzed from the melting peak in various crystallization times, because crystallizaton rates for these block copolymers were so slow that the exothermal peak in crystallization could not be detected clearly.

Spherulites were observed with an optical polarizing microscope (OLYMPUS BHS-705-P) equipped with a calibrated hot stage.

3. Results and discussion

PTHF–PS block copolymers (Block 1, Block 2, Block 3 and Block 4), PTHF homopolymers (Homo 1, Homo 2 and Homo 3) and PTHF/PS blends (Blend 1, Blend 2 and Blend 3) employed for crystallization are listed in Table 1. The precursors of the respective copolymers were used for the samples of a series of homopolymers and blends. The molecular weights and compositions of the constituent homopolymers in Blend 1, Blend 2 and Blend 3 are the same as those of the corresponding block copolymers. The samples were crystallized in the range of T_c indicated in Table 1. Since discrepancy in the DC, for each sample was within 3% in the range of T_c studied here, the average values of DC are shown in Table 1. Apparent equilibrium melting temperatures T_m^0 were obtained from the Hoffman–Weeks plots shown in Fig. 2.

Formation of spherulites was observed for Block 1 as well as a series of homopolymers and blends, while not done for Block 2 and Block 3, but it is not clear whether no observation of spherulites for Block 2 and 3 is due to very small DC or not.

3.1. Crystallizability

As shown in Table 1, the values of DC are smaller in order of homopolymer >blend > block copolymer. In particular, DC of Block 2 and Block 3 is very small, and no melting peak of Block 4 was detected by DSC even in both the crystallization conditions of 3°C, 20 days and −20°C, 7 days, while DC of Block 1 is not so small compared with that of the blends. The behavior of DC in the block copolymers may be due to microphase structure in the melt containing the glassy PS domains. Taking account of the copolymer composition, the PTHF component of Block 1 exists as a matrix while PTHF in Block 2 and Block 3 may be located in the lamellar or cylindrical domain, that is, in the semidiscontinuous domain. The PTHF domain of Block 4 may be spherical, i.e. discontinuous.

Further investigations on crystallizability of Block 4 were carried out for its blends with the PTHF homopolymer whose molecular weights were 2.7×10^3, 4.0×10^3 and 1.0×10^4, respectively. Degrees of crystallinity on the same crystallization condition as that for Homo 1–3 were about 50% for all the pure PTHF homopolymers added. As shown in Table 2, crystallizability can be classified into three types: (1) the blends do not crystallize in the total PTHF content less than about 40%; while (2) the blends crystallize a little in 40–50% contents; and (3) in the content more than 50% the blends crystallize as much as the homopolymer blends shown in Table 1. This tendency is parallel to that of the neat block copolymers. The increase of DC in case (3) may be due to macrophase separation caused by addition of the homopolymer. Cases (1) and (2), which

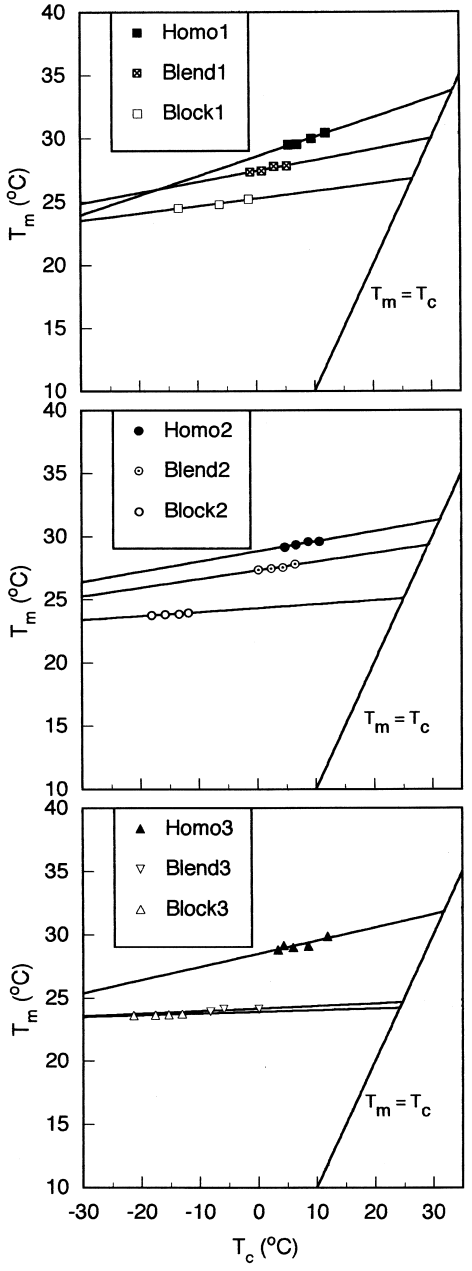

Fig. 2. Hoffman–Weeks plots.

correspond to crystallizability of neat Block 4 and Block 2, 3, respectively, may come from the fact that crystallization is restricted by the microphase separation structure kept even in blending. Here it should be noted that crystallization did not occur in case (1). This suggests that even the homopolymer cannot crystallize in the situation that the polymer is dissolved in the island-like microdomain.

In both Block 4 and the above case (1) the PTHF segments are located in the island-like microdomain surrounded by the glassy PS matrix. Nojima et al. [22] found that poly(ϵ-caprolactone) (PCL) segments in the block copolymer composed of PCL and cross-linked poly (butadiene) could crystallize even within the island-like

Table 2
Degree of crystallinity in the blends of Block 4 with PTHF homopolymer

Sample[a]	PTHF cont.		DC (%)[b]	
	(vol%)[c]	(Homo%)[d]	3°C/20 days	− 20°C/7 days
2.7-Bld	33	9	–	–
	35	17	–	–
	38	23	–	–
	41	33	3	0.5
	48	50	4	0.2
4-Bld	38	23	–	–
	41	33	–	–
	48	50	2	0.3
	58	67	32	33
10-Bld	33	9	–	–
	41	33	–	–
	48	50	5	5
	58	67	18	25

[a] "*n*" in sample name *n*-Bld indicates $n \times 10^3$ for the molecular weight of the PTHF homopolymer added to Block 4.
[b] "–" indicates that the melting peak was not detected by DSC.
[c] The total content of PTHF in the blend.
[d] The fraction of the PTHF homopolymer in the total amount of PTHF.

domain. It has been reported so far that the weekly segregated microphase separation structure is easily destroyed by crystallization [1–3]. Although PCL-*block*-poly(butadiene) is such a kind of copolymer, the microphase structure is fixed by cross-linking. The different point between the copolymers employed by Nojima et al. and us is whether the island-like domain is surrounded by the rubbery or glassy matrix, namely whether the shape of the domain is flexibly changeable or not. Therefore, it is concluded from both ours, and their results, that it is very difficult to crystallize inside a *rigid* island-like microdomain. Kaji and coworkers [23–26] demonstrated that spinodal decomposition occurred in the induction period of crystallization and that the wave length of the density fluctuation was 20–30 nm in the glass crystallization of poly(ethylene telephtalate) (PET) and poly(ethylene naphthalate) (PEN) and the order of microns in the melt crystallization of PET. Even if the wave length of the fluctuation of PTHF is shorter than that of PET and PEN, it may be very difficult that such fluctuation occurs within the rigid spherical microdomain. Alternatively, noncrystallizability in the rigid microdomain may be attributed to another reason, as discussed later, that higher activation energy in crystallization may be required.

3.2. Crystallization kinetics

The Avrami formulation at small degrees of crystallinity is given by [27]

$$X_t = K_n t^n \tag{1}$$

where X_t is the crystallinity at crystallization time t, K_n the overall crystallization rate constant and n the Avrami

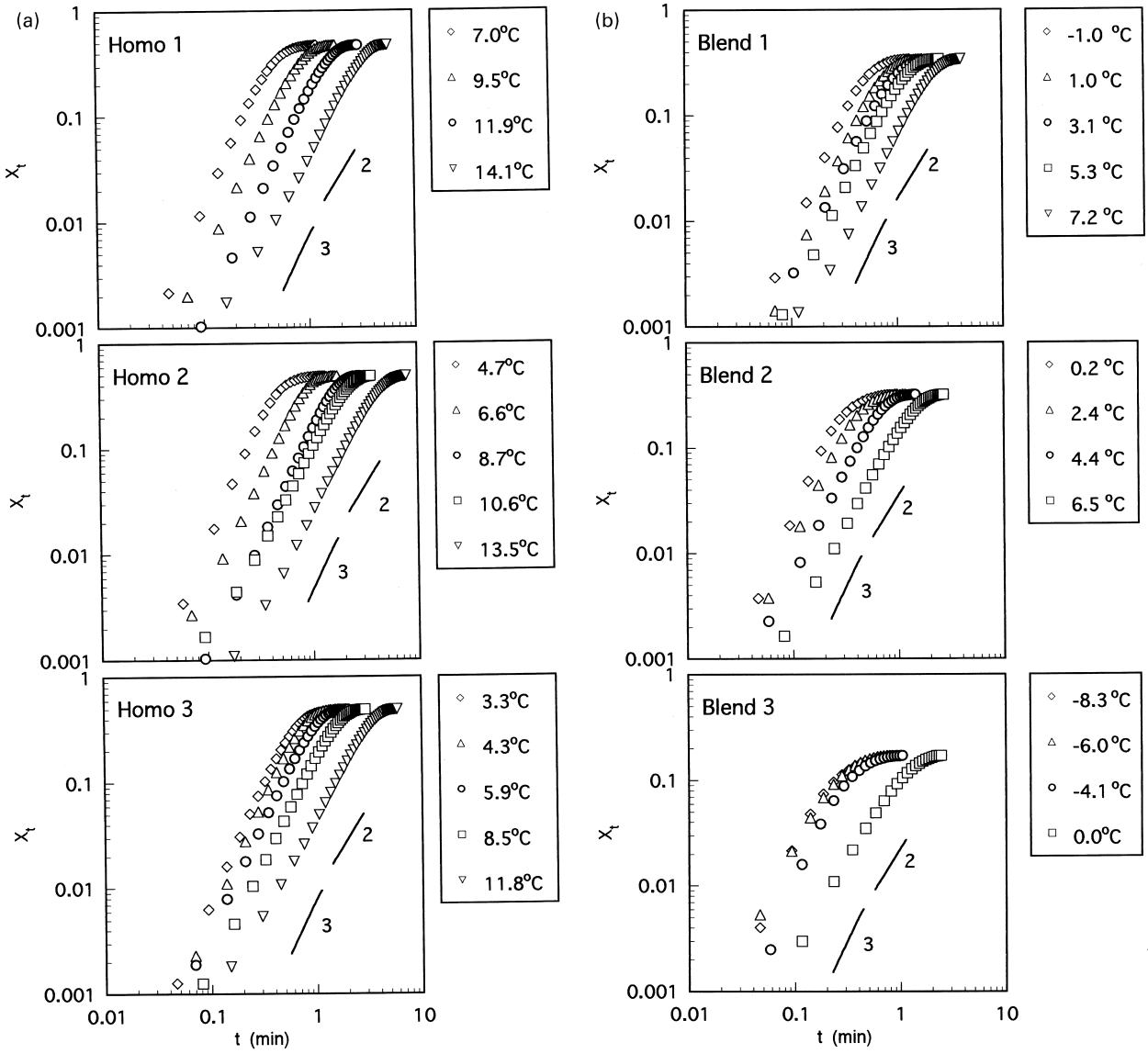

Fig. 3. Crystallization isotherms at the indicated temperatures for: (a) PTHF homopolymers; (b) PTHF/PS blends; and (c) PTHF–PS block copolymers.

exponent. Fig. 3 shows plots of logarithms of crystallinity against crystallization time. The exponents n obtained from the initial slope of the plots are summarized in Table 3. The values of n for the blends are not different from those for the homopolymers. Block 1 also has the almost same n value. On the other hand, n for Block 2 and Block 3 is extremely small. Sakurai et al. [28] also found a small n value for diblock copolymer/homopolymer blends with a small composition of the crystalline component. Their discussion about such a small n is as follows: "a lower geometric dimensionality in the microdomain should give a higher spatial constraint, which means a lower dimensionality in the crystallization growth and therefore a lower value of the Avrami exponent". In our block copolymers Block 2 and Block 3 the microdomain structure may be lamellar and/or cylindrical, respectively, and the microdomains are surrounded by glassy PS. Therefore, PTHF in Block 2 and Block 3 must crystallize under a high spatial constraint, which leads to a smaller n value. In Block 1, on the other hand, crystallization is not constrained because the PTHF component is located as a matrix in the melt, and therefore n is not different from that of the homopolymers and blends.

Another striking feature in crystallization kinetics of the block copolymers is shown in Fig. 4. The linear overall rate constant is expressed as $K_n^{1/n}$. Fig. 4 shows Arrhenius-type plots of $K_n^{1/n}$ against the reciprocal of supercooling degree ΔT, where K_n was estimated at 3% crystallinity using the following equation derived from Eq. (1):

$$(1/n)\ln K_n = (1/n)\ln X_t + \ln(1/t) \quad (2)$$

As shown in Fig. 4, the linear rate constants of the block copolymers, in particular Block 2 and Block 3, are much smaller than those of the homopolymers, while those of the blends are almost the same as those of the homopolymers.

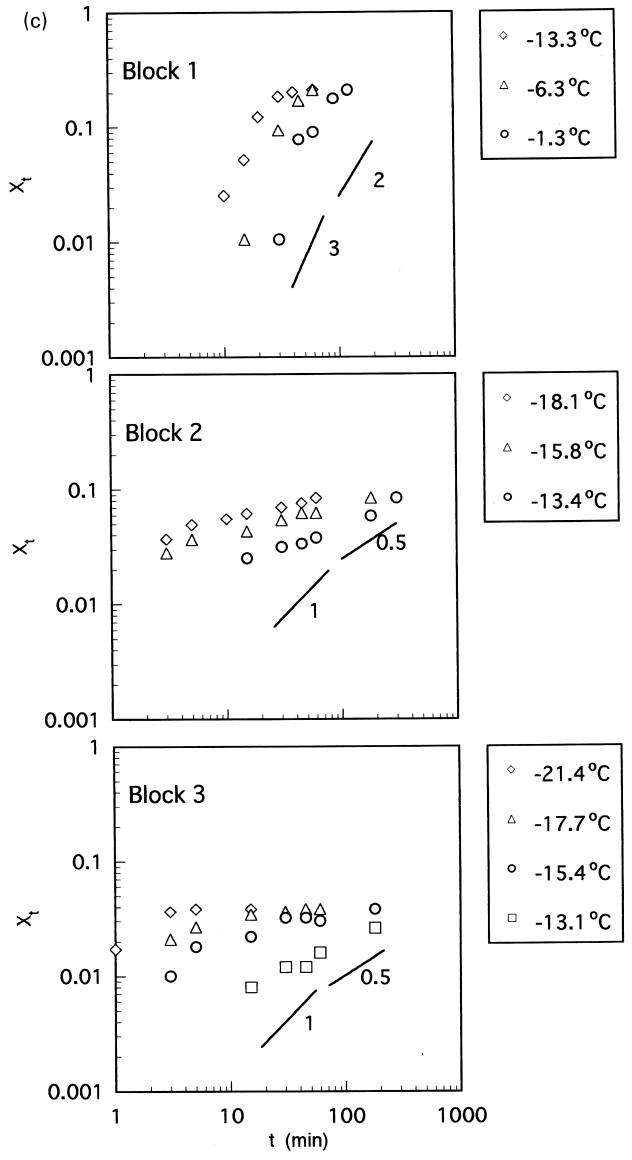

Fig. 3. (*continued*)

Furthermore, the slope of the plots are much steeper for Block 2 and 3 than for Block 1 whose slope is almost the same as that for the blends and homopolymers. The slope corresponds to apparent activation energy of crystallization. The high activation energy of Block 2 and Block 3 may be caused by the fact that the crystallization must occur inside a restricted rigid space such as cylindrical or lamellar microdomain surrounded by glassy PS. This effect is larger for Block 4 in which no crystallization was observed, than for Block 2 and Block 3, because the cylindrical and lamellar domains are open toward one and two dimensional directions, respectively, while the spherical domain is closed to any direction. In Block 1, on the other hand, the island-like PS domain can move in the process of the crystallization of PTHF, which leads to a slower crystallization rate but not higher activation energy.

Table 3
Avrami index and overall rate constant

Sample	T_c (°C)	n	K_n (min^{-n})
Homo 1	7.0	2.3	2.00
	9.5	2.2	6.17×10^{-1}
	11.9	2.2	1.76×10^{-1}
	14.1	2.0	4.06×10^{-2}
Homo 2	4.7	2.4	2.08
	6.6	2.1	6.47×10^{-1}
	8.7	2.1	1.57×10^{-1}
	10.6	1.8	1.24×10^{-1}
	13.5	2.0	2.40×10^{-2}
Homo 3	3.3	2.3	1.04
	4.3	2.3	7.38×10^{-1}
	5.9	2.1	4.78×10^{-1}
	8.5	2.0	1.96×10^{-1}
	11.8	1.9	4.66×10^{-2}
Blend 1	−1.0	2.3	2.65
	1.0	2.2	5.68×10^{-1}
	3.1	2.0	3.76×10^{-1}
	5.3	2.1	2.30×10^{-1}
	7.2	2.0	6.81×10^{-2}
Blend 2	0.2	2.3	3.17
	2.4	2.1	1.86
	4.4	2.0	7.69×10^{-1}
	6.5	1.9	2.05×10^{-1}
Blend 3	−8.3	2.3	3.02
	−6.0	2.0	3.06
	−4.1	2.2	1.49
	0.0	1.9	2.07×10^{-1}
Block 1	−13.3	2.2	1.19×10^{-4}
	−6.3	2.2	2.53×10^{-5}
	−1.3	2.4	6.54×10^{-6}
Block 2	−18.1	0.56	2.08×10^{-2}
	−15.8	0.52	1.62×10^{-2}
	−13.4	0.47	5.91×10^{-3}
Block 3	−21.4	0.53	1.83×10^{-2}
	−17.7	0.47	1.18×10^{-2}
	−15.4	0.44	5.89×10^{-3}
	−13.1	0.47	1.90×10^{-3}

The temperature dependence of activation energy in crystallization can be expressed by the Lauritzen–Hoffman theory [29–31]. According to the theory, the crystallization rate G can be written as

$$G = G_0 \exp(-\Delta E/RT_c) \exp(-\Delta\Phi/RT_c) \quad (3)$$

where G_0 is a constant, ΔE the activation energy of transport and $\Delta\Phi$ the free energy for nucleation which is expressed as

$$\Delta\Phi = k_i b_0 \sigma_e \sigma_s T_m^0 / \Delta H_f \Delta T \quad (4)$$

in which k_i is the constant to be taken as 4, 2 and 4 for Regimes I, II and III, respectively, b_0 is the distance between two adjacent fold planes, σ_s and σ_e are the lateral and end surface free energies, respectively, and ΔH_f is the enthalpy of fusion per unit volume. G is related to the rate constant K_n

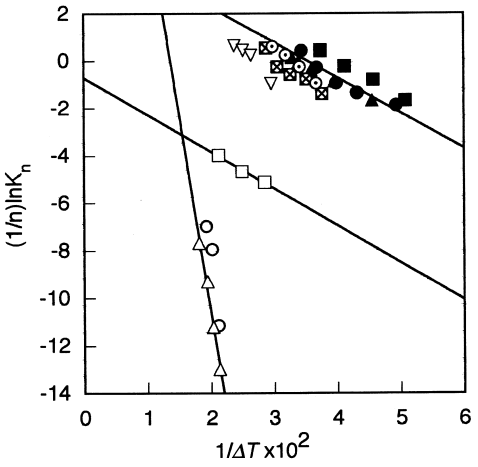

Fig. 4. Arrhenius type plots of the linear overall rate constant of crystallization vs. the reciprocal of the supercooling degree. The symbols are the same as those in Fig. 2.

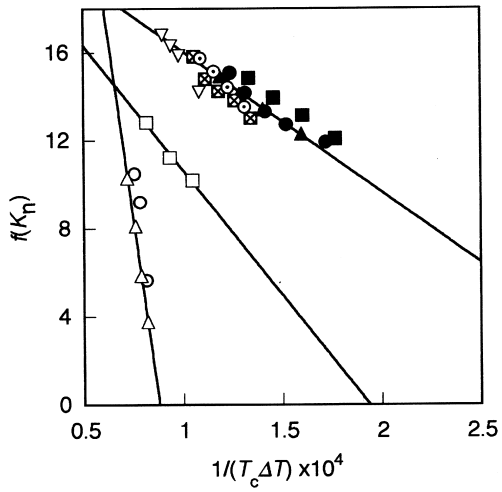

Fig. 5. Plots of the quantity $f(K_n)$ versus $1/(T_c\Delta T)$. The symbols are the same as those in Fig. 2.

as follows:

$$\ln G \sim (1/n) \ln K_n \tag{5}$$

Putting $f(K_n)$ as

$$f(K_n) = (1/n) \ln K_n + \Delta E/\mathrm{R}T_c \tag{6}$$

the following equation can be obtained from Eqs. (3)–(5):

$$f(K_n) \sim k_i b_0 \sigma_e \sigma_s T_m^0/(\Delta H_f \Delta T \mathrm{R} T_c) \tag{7}$$

Then, the plots of $f(K_n)$ against $1/(T_c\Delta T)$ give the temperature dependence of the nucleation term. Here the WLF type was assumed for the transport energy, i.e.

$$\Delta E = C_1 T_c/(C_2 + T_c - T_g) \tag{8}$$

where C_1 and C_2 was taken as 4120 cal mol^{-1} and 51.6 K, respectively.

Fig. 5 shows the plots thus obtained. The slope can be related to both the surface free energy and the index dependent on Regime as seen in Eq. (7). Taking into account that the spherulites were observed for the homopolymers, blends and Block 1, their Regimes may be II, while it is not clear for Block 2 and 3 whether their Regime is II or III because the supercooling degrees are significantly large. In Table 4 are shown the values of the surface free energy estimated from relation (7) using $b_0 = 8.90 \times 10^{-8}$ cm [32] and $\Delta H_f = 1.91 \times 10^9$ erg cm^{-3} [21]. The surface free energy is much larger for Block 2 and 3 than for Homo's, Blend's and Block 1. The ratios of the square root of $\sigma_s\ \sigma_e$ for (Block 2, 3) to (Homo, Blend) and Block 1 are 3.1 and 2.4, respectively.

One of the reasons for such large surface free energy for Block 2 and 3 may be that the segment density in the amorphous region of PTHF is lowered by volume shrinkage occurring with crystallization inside the restricted rigid space, which leads to high free energy at the interface between the crystal and melt. The relation between the surface tension γ and density ρ has been expressed by MacLeod's equation [33]:

$$\gamma \propto \rho^n \tag{9}$$

where n is a constant independent of temperature and has been estimated to be 3.3 for the melt of PTHF [20]. An example of lowering of γ obtained from Eq. (9) is as follows. The extrapolations of the surface tension γ_a and density ρ_a measured in the melt state [20] gives $\gamma_{a1} =$ 33 dyn/cm and $\rho_{a1} = 1.002$ g/cm^3, respectively, at 0°C, while γ_{a2} is 25 dyn/cm at a lower density, $\rho_{a2} = 0.912$, when 50 wt% PTHF crystallizes inside the restricted space, where ρ_{a2} of the melt at a crystallinity of x under a constant volume was estimated using

$$x/\rho_c + (1 - x)/\rho_{a2} = 1/\rho_{a1} \tag{10}$$

in which ρ_c is the density of the crystal and taken as $\rho_c =$ 1.112 [32]. Such a decrease in ρ_{a2} of the melt may bring higher interfacial free energy between the crystal and melt. Simultaneously, free energy at the interface between the glassy PS and melt PTHF may be increased, and also lowering of the density in a local portion leads to higher potential energy of the system, although these effects are not included explicitly in Eq. (3). In Block 2 and 3, however, the lowering of the melt density does not appear so much at least from a static point of view, because the final DC is less than 10% as shown in Table 1. Therefore, if the high interfacial free energy is caused by the density lowering, it may be attributed to the lowering of the density occurring locally in the vicinity of the interface in the process of nucleation.

If the high surface free energy or activation energy is brought from another fact such as the density fluctuation in the induction period of crystallization as discussed in the previous subsection, then the high free energy obtained from Eq. (7) is just an apparent one, and the specific situation in crystallization of these block copolymers is out of the theory which expresses the activation energy of nucleation

Table 4
Surface free energy

Sample	$\sigma_s\sigma_e$ (erg^2/cm^4)		$(\sigma_s\sigma_e)^{1/2}$ (erg/cm^2)	
	Regime II	(Regime III)	Regime II	(Regime III)
Homo, Blend	309		18	
Block 1	548		23	
Block 2, 3	3180	(1590)	56	(40)

only in Eq. (4). Further investigations and consideration on the crystallization inside the restricted space will be desired.

Acknowledgements

This work was supported by a Grant-in-Aid for Scientific Research (11450365) from the Ministry of Education, Science, Sports, and Culture, Japan and by the Mitsubishi Foundation.

References

[1] Nojima S, Kato K, Yamashita S, Ashida T. Macromolecules 1992;25:2237.
[2] Ryan AJ, Hamley LW, Bras W, Bates FS. Macromolecules 1995;28:3860.
[3] Rangarajan P, Register RA, Fetters LJ, Bras W, Naylor S, Ryan AJ. Macromolecules 1995;28:4932.
[4] Douzinas KC, Cohen RE. Macromolecules 1992;25:5030.
[5] Rangarajan P, Register RA, Adamson DH, Fetters LJ, Bras W, Naylor S, Ryan AJ. Macromolecules 1995;28:1422.
[6] Hamley IW, Fairclough JPA, Terrill NJ, Ryan AJ, Lipic PM, Bates FS, Towns-Andrews E. Macromolecules 1996;29:8835.
[7] Quiram DJ, Register RA, Marchand GR. Macromolecules 1997;30:4551.
[8] Quiram DJ, Register RA, Marchand GR, Ryan AJ. Macromolecules 1997;30:8338.
[9] Herman J-J, Jerome R, Teyssie P, Gervais M, Gallot B. Makromol Chem 1981;182:997.
[10] Heuschen J, Terome R, Teyssie P. J Polym Sci, Polym Phys Ed 1989;27:523.
[11] Balsams V, Gyldenfeldt F, Stadler R. Makromol Chem 1996;197:3317.
[12] Nojima S, Kakihira H, Tanimoto S, Nakatani H, Sasaki S. Polym J 2000;32:75.
[13] Nojima S, Tanaka H, Rohadi A, Sasaki S. Polymer 1998;39:1727.
[14] Gervais M, Gallot B. Polymer 1981;22:1129.
[15] Liu LZ, Li H, Jiang B, Zhou E. Polymer 1994;35:5513.
[16] Liu LZ, Jiang B, Zhou E. Polymer 1996;37:3937.
[17] Liu LZ, Yeh F, Chu B. Macromoleules 1996;29:5336 (density of PTHF).
[18] Liu LZ, Xu W, Li H, Su F, Zhou E. Macromolecules 1997;30:1363.
[19] Zoller P. In: Brandrup J, Immergut EH, editors. 3rd ed. Polymer handbook, Chap. VI, Table B4. New York: Wiley, 1989 (A).
[20] Roe R-J. J Colloid Interface Sci 1969;31:228.
[21] Clegg GA, Gee KR, Melia TP, Tyson A. Polymer 1968;9:501.
[22] Nojima S, Hashizume K, Rohadi A, Sasaki S. Polymer 1997;38:2711.
[23] Imai M, Mori K, Mizutani T, Kaji K, Kanaya T. Polymer 1992;33:3451.
[24] Imai M, Kaji K, Kanaya T, Sakai Y. Phys Rev B 1995;52:12 696.
[25] Matsuba G, Kanaya T, Saito M, Kaji K, Nishida K. Phys Rev E 2000;62:R1497.
[26] Kaji K, Nishida K, Matsuba G, Kanaya T, Yamamoto H, Saito M, Imai M. Polym Prepr Jpn 1999;48:3420.
[27] Alamo RG, Mandelkern L. Macromolecules 1991;24:6480.
[28] Sakurai K, MacKnight WJ, Lohse DJ, Shulz DN, Sissano JA. Macromolecules 1994;27:4941.
[29] Hoffman JD, Davis GT, Lauritzen Jr JI. In: Hannay NB, editor. Treatise on solid state chemistry, vol. 3. New York: Plenum Press, 1976 (chap. 7).
[30] Hoffman JD. Polymer 1982;23:656.
[31] Hoffman JD. Polymer 1983;24:3.
[32] Tadokoro H. J Polym Sci, Part C 1996;15:1.
[33] Wu S. J Macromol Sci C 1974;10:1.